Subsurface Sensing Technologies and Applications Vol. 2, No. 2, 2001

FTIR Microscopic Studies on Normal, Polyp, and Malignant Human Colonic Tissues

Jagannathan Ramesh*, Ahmad Salman*, and Shaul Mordechai*

Department of Physics, Ben-Gurion University, Beer-Sheva 84105, Israel

Shmuel Argov, Jed Goldstein, and Igor Sinelnikov

Department of Pathology, Soroka University Medical Centre, Beer-Sheva 84105, Israel

Shlomo Walfisch

Colorectal Unit, Soroka University Medical Center, Beer-Sheva 84105, Israel

Hugo Guterman

Department of Electrical and Computer Engineering, Ben Gurion University, Beer-Sheva 84105, Israel

Received Sept. 17, 2000; Revised Jan. 29, 2001

Fourier-Transform Infrared Spectroscopy (FTIR) employs a unique approach to optical diagnosis of tissue pathology based on the characteristic molecular vibrational spectra of the tissue. The biomolecular changes in the cellular and sub-cellular levels developing in abnormal tissue, including a majority of cancer forms, manifest themselves in different optical signatures, which can be detected in infrared microspectroscopy. This report has two parts. In the first part, we report studies on normal, premalignant (polyp) and malignant human colonic tissues from three patients with different stages of malignancy. Our method is based on microscopic infrared study (FTIR-microscopy) of thin tissue specimens and a direct comparison with traditional histopathological analysis, which serves as a ''gold'' reference. The limited data available showed normal colonic tissue has a stronger absorption than polypoid tumor and cancerous types over a wide region in a total of 100 measurements. Detailed analysis showed that there is a significant decrease in total carbohydrate, phosphate and possibly creatine contents for polyp and cancerous tissue types in comparison to the controls. The same trend is maintained in seven other patients studied. The second part consists of an analysis showing the influence of various independent factors such as age, sex and grade of malignancy. Our preliminary

*To whom all correspondence should be addressed. E-mail: shaulm@bgumail.bgu.ac.il

1566-0184/01/0400-0099$19.50/0

results suggest that among the above three factors, age and grade of malignancy have significant effect on the metabolites level, but sex has only minor effect on the measured spectra. Initial results on Linear Discriminant Analysis (LDA) showed good classification between normal and malignant cells of human colonic tissues.

Key Words. Colon cancer, FTIR microscopy, polyp, age, grade of malignancy, LDA.

1. Introduction

Of the estimated 5.2 million deaths from cancer per year in the world, 55% (2.8 million) occurs in developing countries. Lung cancer is still the most common cause of death from cancer worldwide with over 900,000 deaths per year, followed by gastric cancer with over 600,000 deaths and colorectal and liver cancers accounting for at least 400,000 deaths each [1]. The ACS (American Cancer Society) estimates that there will be 93,800 new diagnoses of colon cancer and 36,400 new diagnoses of rectal cancer in the year 2000 in the U.S. [2]. Despite the improvement in diagnostic techniques, the vast majority of pancreatic cancers, more than 90%, have either advanced or metastasized by the time they are diagnosed [3]. Hence there is an urgent need to develop novel non-invasive diagnostic method to detect the malignancy in the earlier stage.

Infrared (IR) spectroscopy is well known for its uniqueness as a non-destructive method in identifying vibrational structure of various materials. The spectra allow measuring complex molecular vibrational modes. Various biomolecular components of the cell give a characteristic IR spectrum, which is rich in structural and functional aspects [4,5]. One of the most promising applications of the IR-based techniques, which has become possible now, is in biomedicine. IR spectroscopy can detect and monitor characteristic changes in molecular composition and structure that accompany transformation from normal to cancerous state [5–8]. This could be done in the early stages of malignancy (e.g., polyp which is called pre-malignant), which are not yet evident in standard methods [9–11]. IR spectroscopy opens new and modern areas of medical research, as it causes no damage to the cells.

We have measured the characteristic microscopic IR spectra of variety of thin sections of normal, polyp and cancerous human intestinal tissues (colon adenocarcinoma) which is one of the major causes of morbidity and mortality. The measured spectroscopic features contain the vital information, which enables us to differentiate the malignant and benign tissues based solely on the measured spectroscopic fingerprints of the tissue. The analysis of limited data on various markers showed that carbohydrate and phosphate levels get significantly reduced in cancerous tissues relative to the controls. In the literature there is no information available on the effect of

age, sex and grade of malignancy on tissue pathology which may be helpful in the tissue diagnostics using optical methods. Hence, we analyzed the FTIR data on ten different patients to understand the effect of age, sex and grade of malignancy. Our initial results showed interesting correlation between young and old patients in terms of biomolecular compositions. Initial results of Linear Discriminant Analysis (LDA) showed that the normal and malignant cells could be identified with about 89% accuracy. Further studies are required to substantiate the above observations.

2. Material and Methods

2.1. Sample Preparation

Formalin-fixed, parafin-embedded tissues from 10 adenocarcinoma patients were retrieved from the histopathology files of Soroka University Medical Center, Beer Sheva (SUMC). The tissue samples used in this study were selected to include normal mucosa, polyp and malignant areas. Two parafin sections were cut from each biopsy, one was placed on zinc-selenium slide and the other on glass slide. The first slide was deparaffinized using xylol and alcohol and was used for FTIR measurements. The second slide was stained with hematoxylin and eosin for histology review.

2.2. FTIR Microspectroscopy

Microscopic FTIR-measurements were performed in transmission mode. For the transmission measurements we used the FTIR microscope IRscope II with MCT detector coupled to the FTIR spectrometer (BRUKER EQUINOX model 55/S OPUS software). The microscope is also equipped with a CCD-camera for the visible range of the spectrum. The measured spectra cover the wavenumber range 600–4000 cm^{-1} in the mid-IR region. Since the ordinary glass slides have strong absorption in the wavelength range of our interest, we used zinc sellenide crystals, which are highly transparent to IR light. One of the major problems encountered in such studies in the past is the contamination, which is possible during tissue preparation. The contamination can mask the spectral differences between normal and cancerous tissues, yielding ambiguous results. To avoid this problem, we have performed our measurements of normal, polyp and cancerous intestinal tissues using a microscopic inspection in parallel with detailed pathological analysis of the tissue architecture. The samples were thin sections of formalin fixed tissues. All three types (normal, polyp and malignant) of the tissue samples were obtained from each patient. Spectra from patients with different cancer grading have been measured using the

same experimental procedure. During each measurement, the measured sites were about $50 \times 50\,\mu m^2$ at most. Such area contains only few cells. The spectrum was taken as an average of 128 scans to increase the signal to noise ratio. Baseline correction for all the spectra was done by dividing the spectra into 64 sections of equal size and then the *y*-value minima of the spectra were connected giving best fit to the background using polynomial function. The spectra were normalized arbitrarily to 2 for the amide I peak at $1643\,cm^{-1}$ after baseline correction for the entire spectrum. For each tissue type the spectrum is taken as the average of five different measurements at various sites of the tissue section.

2.3. Spectral Analysis and Fitting Procedures

Band fitting analysis was performed using the software PEAKFIT (Version 4.0). The measured spectra were fitted using a standard Gaussian peak shape satisfying the following relationship:

$$I(\nu) = I_0 \exp\left[-\frac{1}{2}\left(\frac{\nu - \nu_0}{w}\right)^2 \right] \tag{1}$$

Where, $I(\nu)$ represents the IR absorbance at wavenumber, ν, ν_0 is the centroid of the band and w is the width parameter (12,13). The full width at half maximum (FWHM) of the band Γ is calculated using the relation

$$\Gamma = 2.36w\ (cm^{-1}) \tag{2}$$

With the enhanced resolution achieved due to high signal to noise ratio, the weak absorption bands can be resolved to a greater extent. Firstly, the second derivative spectrum was generated. The second derivative spectrum was used in identifying the hidden peaks. Secondly, the peaks obtained from the second derivative spectrum were fitted allowing the centroids, widths and absorbance values to vary in the process. In addition, a linear function was used to fit the residual background. The above analysis yielded reliable fits for the entire region of the spectra. The integrated intensities were calculated using OPUS software to quantify the metabolites for normal, polyp and malignant tissue samples.

2.4. Linear Discriminant Analysis

To fully evaluate the performance of the proposed method, linear discriminant analysis (LDA) [14] was employed using MATLAB (Version 5.3: Maths Works Inc.). LDA is a classification technique that employs Mahalanobis distance to determine the class of an unknown sample. In this

study, training and test sets were selected randomly from the database. Fifty percent of each set was employed for training and the remainder for test. In addition, the validation experiment was repeated 100 times, with the same input features but with different sets of randomly selected training and test sets, and the results were averaged.

3. Results and Discussion

Figure 1a presents histological cross section image of formalin-fixed human colonic tissue. The thin microvascular vessels pass vertically between crypts in the normal lamina propia. The polyp lesions (Fig. 1b) shows different morphology compared to normal, appearing as pedunculated growths above the surrounding normal tissue surface. The figure displays adenomatous polyp with tubular adenoma. The neoplastic glands are forming tubules. The adenomatous epithelium preserves mucus production-goblet cells. In this field, there is a marked decrease in mucus production. There is focal loss of nuclear polarity, and an increase in nucleocytoplasmic ratio. Figure 1c gives a low power view of adenocarcinoma, a malignant epithelial tumor. The gland shows cribriform pattern, with loss of mucin production and foci of necrotic debris. The adenocarcinoma glands (grade II) are irregular and torous.

Figure 2 shows a typical infrared absorption spectrum of normal, polyp and cancerous human intestinal tissues in the spectral range 600–2000 cm^{-1} for three patients. The patients a, b, and c belong to early, moderate and advanced stages of the malignancy respectively as determined by the pathologist. The spectrum is dominated by two absorbance bands at 1643 and 1544 cm^{-1} known as amide I and II respectively. Amide I arises from the C=O hydrogen bonded stretching vibrations, and amide II from the C–N stretching and a CNH bending vibrations. The intensity differences for normal, polyp and cancerous for amide II band was not significant in all three cases. The weaker aminoacid side chain from peptides and proteins at 1456 and 1401 cm^{-1} are associated with the asymmetric and symmetric CH_3 bending vibrations [15]. The absorption peaks at 1243 and 1075 cm^{-1} are due to the PO_2^- ionized asymmetric and symmetric stretching respectively [1,16]. The absorption due to normal tissue was higher than polyp and cancerous types in this entire region of the spectrum in all three patients. In the case of patient c, intensity changes for phosphate absorption bands between polyp and cancerous were not significant. But, in the case of patient a, the absorption spectrum of polyp was more intensive than the cancerous tissue and it reversed in the case of patient b. No frequency shifts were observed in the entire region (600–2000 cm^{-1}).

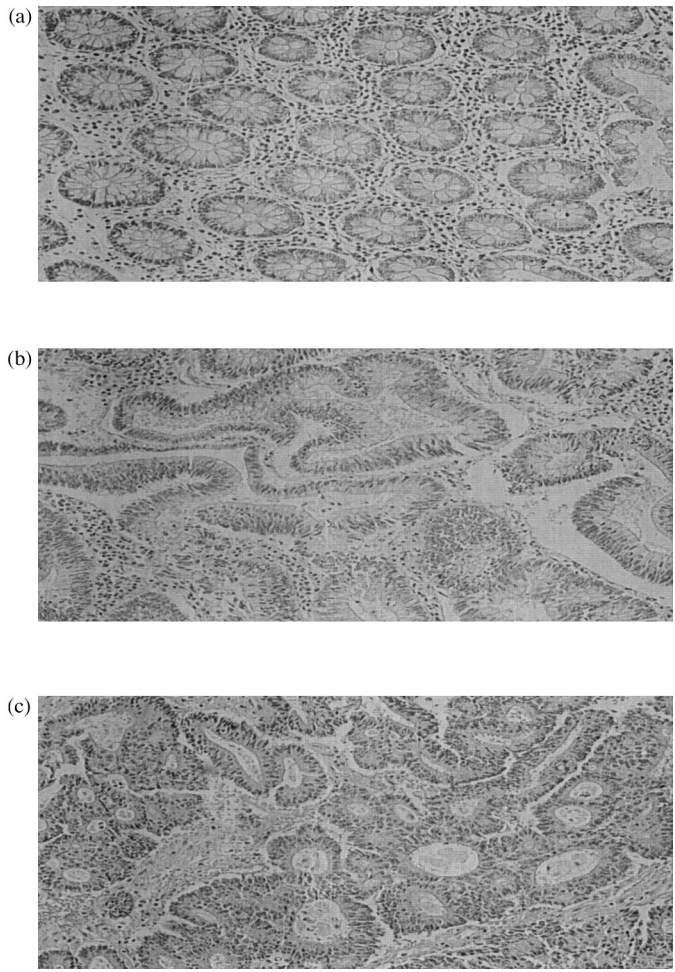

Figure 1. Histological image cross sections of formalin fixed human colonic tissue stained with hematoxylin-teosin; (a) normal, (b) Polyp, (c) malignant.

The bands at 1025 and 1045 cm^{-1} in IR spectra are responsible for the vibrational modes of $–CH_2OH$ groups and the C–O stretching coupled with C–O bending of the C–OH groups of carbohydrates (includes glucose, fructose and glycogen, etc.) [17]. The intensity ratio of the bands at 1045/1545 gives an estimate of the carbohydrate levels, which are shown in Figure 3. The carbohydrate level for normal was higher than polyp and malignant in all three cases. The difference in carbohydrate level between normal and

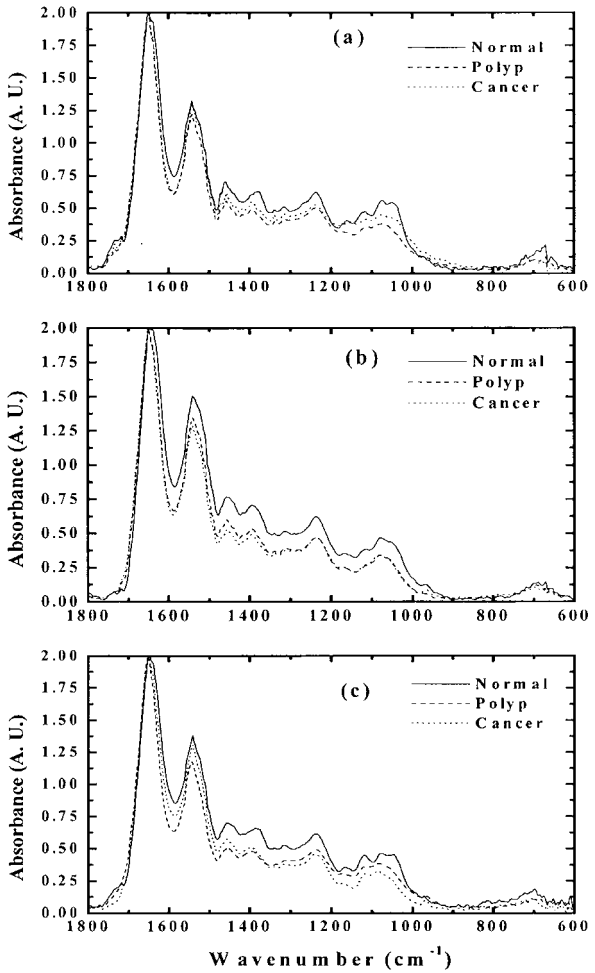

Figure 2. Infrared microspectroscopy in the region 600–1800 cm^{-1} of normal, polyp and malignant tissues of human intestine. (a), (b) and (c) represent the early, moderate and advanced stages of malignancy as reported by the pathologist.

cancer is highest in the patient c who is in the advanced stage. It may be that the carbohydrate absorption or metabolism is affected in cancerous tissue in the advanced stages. In the early case, the carbohydrate content calculated from the spectra, was lower for polyp than the malignant and it reversed in the advanced patient. Here we see good correlation from our spectral analysis, between premalignant and cancerous tissue types for early

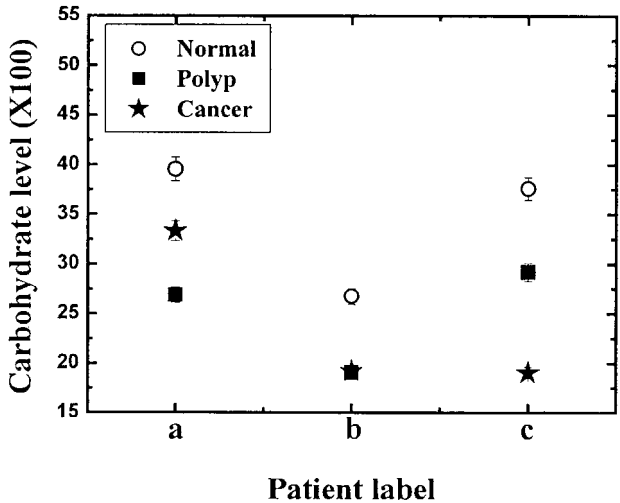

Figure 3. The carbohydrate level taken as the intensity ratio at $(1045/1545) \times 100$ for three patients. In Figures 3–9 the patient labels a, b and c indicate early, moderate, and advanced stages of the malignancy.

and advanced stages. This is not accidental, as in the moderate case the polyp and malignant levels were expected to be the same (average of early and advanced stages) and we found it to be true (patient b).

The phosphate levels reveal the metabolic turnover, as it consists of energy producers such as ATP and GTP and other biomolecular components which include phospholipids, nucleic acids (DNA and RNA) and phosphorylated proteins. The phosphate levels for normal, polyp, and malignant tissues from three patients with different grades of malignancy are shown in Figure 4. Our analysis on limited data showed that the normal tissue had higher phosphate content than polyp and malignant tissues in all three patients. Also, the difference in total phosphate level between normal, polyp and malignant was higher and this enhancement may arise from the fact that phosphate level is the summation of larger number of biomolecules having phosphate group. In early and moderate cases, the phosphate content was higher for polyp than cancerous tissue and it is reversed in the advanced case. But, the difference between polyp and malignant was not significant in all cases. Generally, the informative PO_2^- symmetrical and asymmetrical stretching vibrations, which occur between 1000–1300 cm^{-1}, provide clues to qualitative and quantitative changes for phospholipids and nucleic acids. In our study, the intensity of these vibrations for normal tissue was higher than polyp and cancer types in all three cases. Also, when the

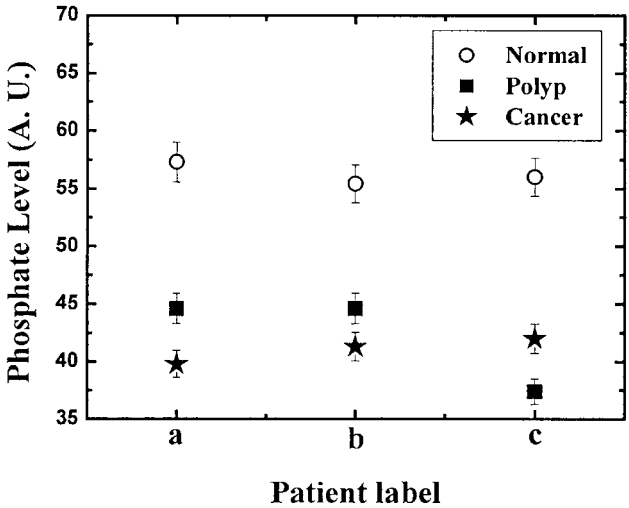

Figure 4. Summed analytic areas of the phosphate bands (symmetric and asymmetric stretching vibrations) for three patients. The analytical areas of the phosphate bands were calculated by using ORIGIN software.

analytical areas for these two phosphate bands were summed up, the same trend was repeated (Fig. 4). The polyp samples showed variations from patient to patient, which may indicate the different stages for polyp before the cell becomes fully transformed. The analysis of phosphate bands arising from symmetric and asymmetric stretching vibration bands, has clearly shown that the total phosphate content is significantly higher in normal tissues than polyp and cancer types.

The ratio of glucose to phosphate was obtained by calculating the intensity ratio at 1030/1080 which is shown in the Figure 5. This scale also provides information on metabolic turnover in the tissues. Our results showed that the glucose/phosphate ratio was higher for normal than polyp and malignant tissues. Similarly in the case of phosphate levels, the difference between normal and the other two tissue types was larger for all three patients.

An increasing absorbance at 1121/1020 ratio from normal to malignant is evident in literature spectra from several different tissues [18]. This is an index of cellular RNA/DNA ratio after subtraction of overlapping absorbancies. The results from our analysis are shown in the Figure 6. In the moderate and advanced cases, the RNA/DNA was higher for malignant tissues than the normal type, which may be a good parameter for diagnostic purposes. It is interesting to note that the difference in ratio between the

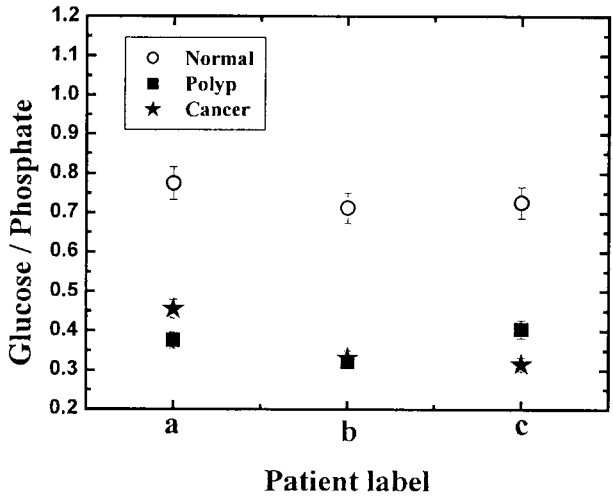

Figure 5. Glucose/phosphate for three patients, calculated by the ratio of intensity at 1030/1080.

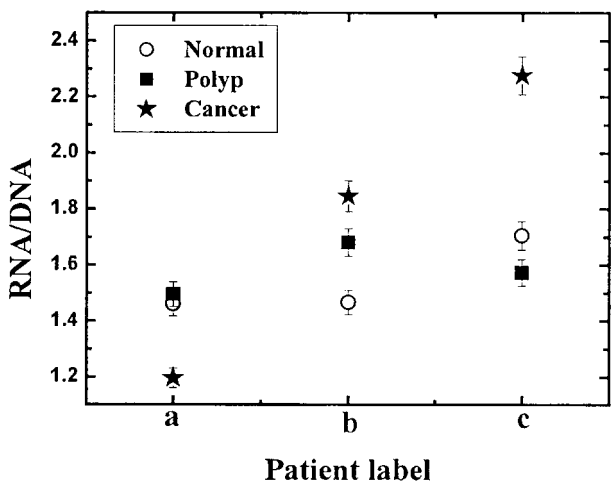

Figure 6. The intensity ratio at 1121/1020 is presented as RNA/DNA for the three patients. The patient labels a, b and c indicates early, moderate and advanced stages of the malignancy.

normal and malignant was very large in the advanced case in comparison to other cases.

Several reports suggest that the amide I/II intensity ratio increase with DNA content of the epithelial cells [19], where as in the case of RBC (Red Blood Cells), the intensity of amide I/II is nearly the same as any other

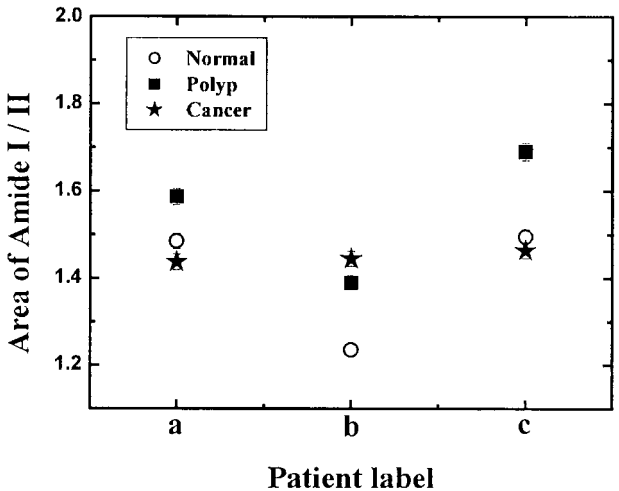

Figure 7. The area of amide I (1643)/II (1544) for three patients.

pure protein spectrum. The ratio of amide I/II is presented in the Figure 7. This ratio was higher for polyp than normal and malignant in two out of three cases (early and moderate). But, the precise reason for this behavior is not clearly understood.

Figure 8 shows the region between 2600–3800 cm^{-1} for three kinds of tissues for three patients. Cholesterol, phospholipids and creatine are the three essential cellular metabolites absorbed between 2800–3500 cm^{-1}. Here also, magnitude of normal tissue was higher than the polyp and cancerous types in all three patients. Since there are symmetric and asymmetric vibrations due to water in the region between 3200–3550 cm^{-1}, hence this region is not considered for analysis. The integrated intensities (for peaks I and II) were calculated by measuring the area under the curve omitting the baseline underneath using OPUS software. The integrated area calculated for the peaks 2848 and 2916 cm^{-1} for three patients is shown in Figure 9a and b. The area for normal tissue was higher than polyp and cancer types in all three cases. The difference between normal and malignant tissue types is larger in early case compared to moderate and advanced cases. The region between 2800–3500 cm^{-1} is due to strong absorption of CH_2, CH_3 stretching

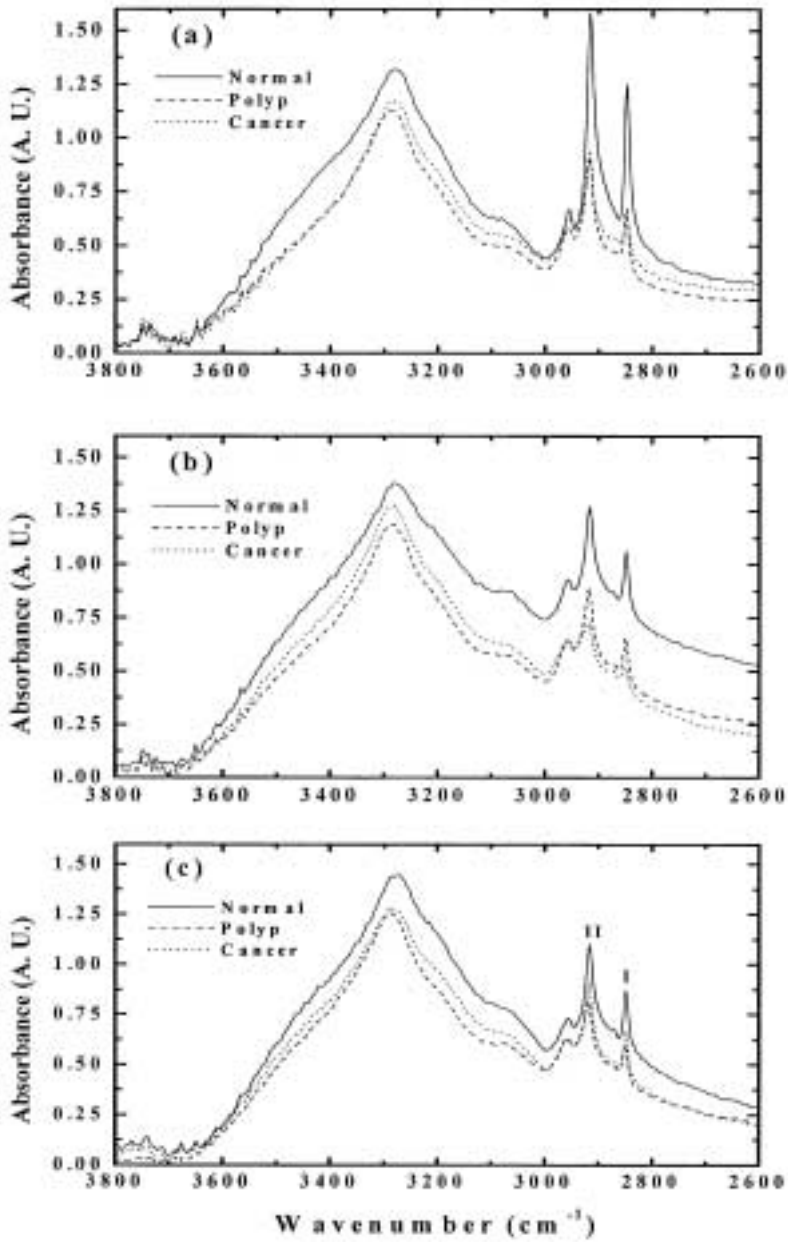

Figure 8. Infrared microspectroscopy in the region 2600–3800 cm^{-1} of normal, polyp and malignant tissue of human intestine.

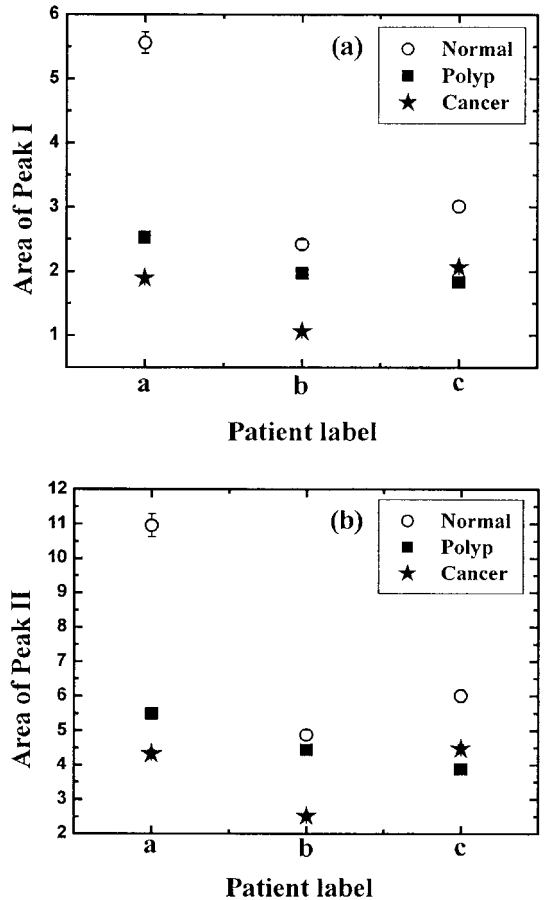

Figure 9. (a) Integrated area of peak I (2848 cm^{-1}), (b) peak II (2916 cm^{-1}) for three patients.

vibrations of phospholipids, cholesterol and creatine. Creatine and cyclocreatine have been shown to inhibit the growth of a variety of human and murine tumors [20]. Antiproliferative effect of creatine is shown to be effective in mice carrying a human colon adenocarcinoma (LS 1747). These results indicate that the creatine levels may be lower in polyp and cancer types compared to normal ones.

Our FTIR investigation on three types of colon tissues for three patients showed that the levels of vital cellular metabolites decrease in polyp and cancer relative to the controls. These results are surprising since other cancer forms e.g., cervical [21], breast [22] and skin cancers [23] show an

increase in the phosphate concentration relative to the normal tissues. Colonic adenocarcinoma shows an entirely different behavior. Our results can be explained by having a better understanding of histogenesis of colonic adenomas. Generally, in normal crypt, the epithelial cells proliferate in the bottom portion and move further with differentiation and finally exit ending up in apoptosis. The recent model given by Moss *et al.* [24] histogenesis of colonic adenomas claims that in adenomas, the proliferation of cells is predominant at lumen and apoptosis at the base, a complete reversal of normal pattern. It is interesting to speculate that the drastic decrease in cellular contents for polyp and cancerous tissues (as shown by our results) can be correlated to the apoptotic stage of polyp and cancerous types. This explains why our results are opposite to the findings for other tissue types. Additional evidences are necessary to substantiate our results by having more FTIR data on samples from different sites of the adenomatous crypt in patients.

The vital parameters such as age, stage of malignancy and sex are not studied in detail in terms of biochemical changes that occur in colon cancer. Hence, we decided to analyze the available FTIR data for ten patients with respect to age and sex. In the group of ten patients studied in detail, there were three young (40–45; patients 3, 6, 9) and seven elderly (70–90) patients. There were six male and four female patients. The various biochemical markers were analyzed to get correlation between the different age and sex groups.

The variation in carbohydrate levels for normal and cancerous tissues for ten patients calculated as the ratio of intensities at 1045/1545 is given in the Figure 10. The analysis provided us with two important results. Firstly, the average carbohydrate content was much lower in malignant tissue of young patients than the elderly ones. The levels for normal samples for both age groups were in the same range indicating that the differences in malignant tissues were true and significant. Secondly, the average carbohydrate content differences between normal and malignant tissues were larger in the cases of moderate stage of malignancy (patient numbers 3–8) compared to early and advanced stages. However, carbohydrate levels did not change considerably between males and females.

Figure 11 presents the variation in phosphate level for two tissue types for ten patients. The phosphate levels were found to be lower in cancerous tissues in younger compared to elderly patients. The change in carbohydrate contents is expected to have impact on phosphate levels as the energy metabolism governs the synthesis of various metabolites containing phosphate group. Our results are in good agreement with this point.

As mentioned before RNA/DNA is a good marker for grading of the malignancy in patients. Our analysis of RNA/DNA for ten patients

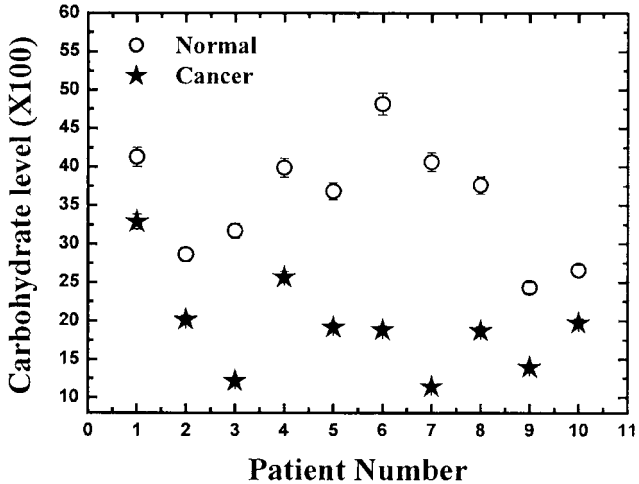

Figure 10. The carbohydrate level taken as the intensity ratio at $(1045/1545) \times 100$ for ten patients. In Figures 10–12 the patient Nos. 1, 2–7 and 8–10 belong to early, moderate and advanced stages of the malignancy.

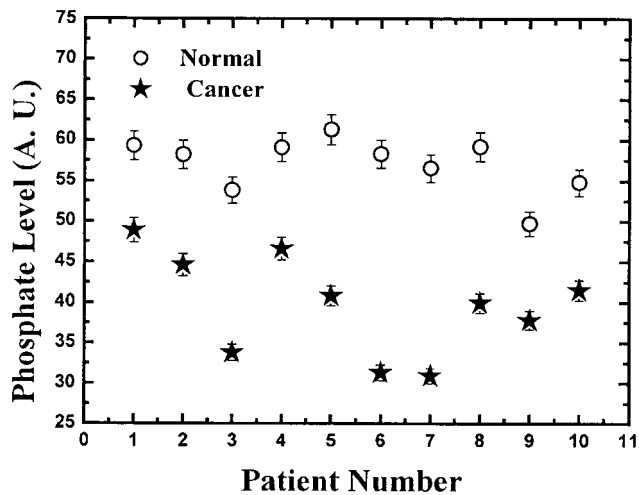

Figure 11. Summed analytic areas of the phosphate bands (symmetric and asymmetric stretching vibrations) for ten patients.

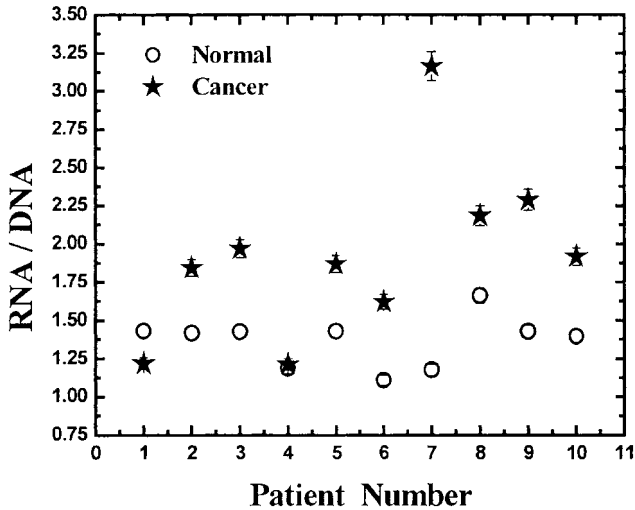

Figure 12. The intensity ratio at 1121/1020 is presented as RNA/DNA for the ten patients.

(Fig. 12) showed that the advanced patients have the highest RNA/DNA in their malignant tissues. This is clear in the case of patient numbers 8, 9, 10 and also the RNA/DNA is higher for cancerous tissue than the normal samples in all ten patients.

Here we present a case study where the specific patient cases are analyzed in detail. Patient number 9 is young in the advanced stage of malignancy having lowest phosphate level in the normal tissue, highest RNA/DNA and lowest carbohydrate content in the malignant tissue. In the patient number 1 (exactly opposite to patient No. 9) who is elderly in the early stage of malignancy was found to have highest phosphate level in the normal tissue, lowest RNA/DNA and highest carbohydrate content in the malignant tissue. The comparison between patient number 1 (old and early stage of malignancy) with patient number 6 (young and moderate stage of malignancy) also followed the same trend as discussed in the previous one. This data shows that there is a perfect correlation between age and stage of malignancy and the composition of different biomolecular components in the tissue of colon cancer patients. Similarly, the patient number 6 who is young having moderate stage of colon cancer was found to display the largest difference in carbohydrate and phosphate levels between normal and malignant tissues, whereas patient number 4, old being in the moderate stage showed the reversal of this trend. This also confirms that age has significant effect on different biochemical markers studied in the case of

colon cancer patients using FTIR microscopy. To substantiate this point, it is essential to do a detailed study comprising larger number of patients which is currently in progress in our laboratory.

The preliminary results of LDA are highly encouraging in discriminating normal from malignant cells. The probabilities of classification using seven sets of features for normal and cancer tissues showed that the best results were obtained for set 1 (phosphate bands having both symmetric and asymmetric) with a success rate of 86.2% and 91.6% for normal and cancer tissue, respectively. Although the success rate of the LDA based classifier is high, a careful analysis reveals about 8.4% of the cancer cases might be classified as normal while up to 13.8% of the normal cases might be classified as cancer. Detailed computational work is in progress in our laboratory to evaluate the different methods of analysis to achieve high sensitivity and specificity.

4. Summary and Conclusions

The results obtained on limited data reported in this study support the idea that major biochemical changes are taking place in the cells undergoing transformation from normal to cancerous state. Cancerous colonic epithelial cells show a systematic decrease in total carbohydrate, phosphate and possibly creatine contents. It seems that the phosphate stretching modes could be useful as infrared spectroscopic markers to discriminate between spectra of normal and cancerous colonic tissues. Also, it is important to identify the special patterns of vibrational modes characteristic to various states of malignancy. With even limited number of patients it could be shown that age and stage of malignancy have dramatic effect on FTIR markers reported in this study. Such study (currently underway by our group) is essential for evaluating the potential of IR microscopy as a new tool for early detection of cancer and to get a better insight on the differences between normal and cancerous cells. Our initial results on mathematical analysis of FTIR spectra on normal and malignant tissue samples showed good classification giving room for detailed investigation in the future.

Acknowledgments

This research work was supported by the Middle East Cancer Consortium (MECC) and the Cancer Research Foundation at the Soroka Medical Center in Memory of Professor Tabb. Many thanks are due to Dr. V. Erukhimovitch for data collection. Discussions with Dr. Mahmoud Huleihel and Dr. B. Cohen are gratefully acknowledged.

References

1. Pisani, P., Parkin, D.M., Bray, F., and Ferlay, J., 1999, Estimates of the worldwide mortality from 25 cancers in 1990, Int. J. Cancer, v. 83, p. 18–29.
2. Ries, L.A., Wingo, P.A., Miller, D.S., Howe, H.L., Weir, H.K., Rosenberg, H.M., Vernon, S.W., Cronin, K., and Edwards, B.K., 2000, The annual report to the nation on the status of cancer 1973–1997, with a special section on colorectal cancer, Cancer, v. 88, p. 2398–2424.
3. Adams, J.T., Poulter, C.A., and Pandya, K.J., 1983, *in* Philip, R., ed., Clinical oncology, sixth edition, published by American Cancer Society, New York.
4. Mantsch, H.H. and Chapman, D., eds., 1996, Infrared Spectroscopy of Biomolecules, John Wiley, New York.
5. Jackson, M., Kim, K., Tetteh, J., Mansfield, J.R., Dolenko, B., Somorjai, R.L., Orr, F.W., Watson, P.H., and Mantsch, H., 1998, Cancer diagnosis by Infrared Spectroscopy: Methodological Aspects, SPIE, v. 3257, p. 24–34.
6. Afanasyeva, N.I., Kolyakov, S.F., Artjushenko, S.G., Sokolov, V.V., and Frank, G.A., 1998, Minimally invasive and *ex vivo* diagnostics of breast cancer tissues by fiber optic evanescent wave Fourier Transform IR (FEW-FTIR) Spectroscopy, SPIE, v. 3250, p. 140–146.
7. Diem, M., Boydston-White, M. S., and Chiriboga, L., 1999, Infrared spectroscopy of cells and tissues: shining light on to a novel subject, Applied Spectroscopy, v. 53, p. 148–161.
8. Franck, P., Nabet, P., and Dousset, B., 1998, Applications of Infrared Spectroscopy to medical biology, Cell. Mol. Biol. v. 44, p. 273–275.
9. Yazdi, H.M., Bertrand, M.A., and Wong, P.T.T., 1996, Detecting structural changes at the molecular level with Fourier transform infrared spectroscopy, Acta Cytologica, v. 40, p. 664–668.
10. Binding, U., Wasche, W., Liebold, K., Winter, H., Gross, U.M., Frege, P., and Muller, G., 1998, Tissue diagnostics by using fiberoptic FTIR-spectroscopy, SPIE, v. 3568, p. 38–45.
11. Cohenford, M.A., Godwin, T.A., Cahn, F., Bhandare, P., Caputo, T.A., and Rigas, B., 1997, Infrared Spectsoscopy of normal and abnormal cervical smears: evaluation by principal component analysis, Gynecologic Oncology, v. 66, p. 59–65.
12. Lucassen, G.W., Caspers, P.J., Pupples, G.J., 1998, *In vivo* infrared and Raman spectroscopy of human stratum corneum, SPIE, v. 3257, p. 52–60.
13. Afanasyeva, N.I., Kolyakov, S.F., and Butvina, L.N., 1998, Remote skin tissue diagnostics *in vivo* by fiber optic evanescent wave Fourier transform infrared (FEW-FTIR) spectroscopy, SPIE, v. 3257, p. 260–266.
14. Haaland, D.M., Jones, H.D.T., and Thomas, E.V., 1997, Multivariate classification of the infrared spectra of cell and tissue samples, Appl. Spectros, v. 51, p. 340–345.
15. Diem, M., 1993, Introduction to modern vibrational spectroscopy, Wiley–Interscience, New York.
16. Krupnik, E., Jackson, M., Bird, R.P., Smith, I.C.P., and Mantsch, H.H., 1998, Investigation into the infrared spectroscopic characteristics of normal and malignant colonic epithelium, SPIE, v. 3257, p. 307–310.
17. Parker, F. S., 1971, Application of infrared spectroscopy in biochemistry, biology, and medicine, Plenum, New York.
18. Andrus, P.G. and Strickland, R.D., 1998, Cancer grading by Fourier transform infrared spectroscopy, Biospectroscopy, v. 4, p. 37–46.
19. Benedetti, E., Bramanti, E., Papineschi, F., and Rossi, I., 1997, Determination of the relative amount of nucleic acids and proteins in leukemic and normal lymphocytes by means of FT-IR microspectroscopy. Appl. Spectrosc, v. 51, p. 792–797.

20. Kristensen, C.A., Askenasy, N., Jain, R.K., and Koretsky, A.P., 1999, Creatine and cyclocreatine treatment of human colon adenocarcinoma xenografts: 31P and 1H magnetic resonance spectroscopic studies, Br. J. Cancer, v. 79, p. 278–285.
21. Chiriboga, L., Xie, P., Yee, H., Zarou, D., Zakim, D., and Diem, M., 1998, Infrared spectroscopy of human tissue. IV. Detection of dysplastic and neoplastic changes of human cervical tissue via infrared microscopy, Cell. Mol. Biol. v. 44, p. 219–229.
22. Dukor, R.K., Liebman, M.N., and Johnson, B.L., 1998, A new, non-destructive method for analysis of clinical samples with FT-IR microspectroscopy. Breast cancer tissue as an example, Cell. Mol. Biol. v. 44, p. 211–217.
23. Wong, P.T.T., Goldstein, S.M., Grekin, R.C., Godwin, T.A., Pivik, C., and Rigas, B., 1993, distinct infrared spectroscopic patterns of human basal cell carcinoma of the skin, Cancer Research, v. 53, p. 762–765.
24. Moss, S.F., Liu, T.C., Petrotos, A., Hsu, T.N., Gold, L.I., and Holt, P.R., 1996, Inward growth of colonic adenomatous polyps, Gastroenterology, v. 111, p. 1425–1432.